**RESEARCH ARTICLE**                                                                                    **Open Access**

# An investigation of Plk1 PBD inhibitor KBJK557 as a tumor growth suppressor in non-small cell lung cancer

Pethaiah Gunasekaran[1,4†], Gong-Hyeon Lee[4†], Yeon Sil Hwang[1], Bon-Chul Koo[1], Eun Hee Han[1], Guel Bang[1], Yeo Kyung La[1], Sunghyun Park[1], Hak Nam Kim[1], Mi-Hyun Kim[2*], Jeong Kyu Bang[1,3,4*] and Eun Kyoung Ryu[1,3*]

**Abstract**

Lung cancer is the second most commonly reported type of cancer worldwide. Approximately 80–85% of lung cancer occurrences are accounted by non-small cell lung cancer (NSCLC). Polo-like kinase-1 (Plk1) plays multiple roles in cell cycle progression and its overexpression is observed in majority of malignancies, including NSCLC. A combination of frontline drugs and inhibitors targeting the Plk kinase domain (KD) has been used to overcome drug resistance in NSCLC. Plk1 KD inhibitors are highly prone to cross-reactivity with similar kinases, eventually leading to undesirable side effects. Moreover, there have been no reports of Plk1 PBD inhibitors showing antitumorigenic effects on NSCLC cells or animal models so far. To address this issue herein, for the first time, our recently reported Plk1 PBD inhibitor KBJK557 was evaluated for the anticancer potential against NSCLC cells. KBJK557 displayed notable cytotoxic effects in A549, PC9, and H1975 cells. Mechanistic investigations revealed that KBJK557-treated cells underwent G2/M cell cycle arrest, triggering subsequent apoptosis. In vivo antitumorigenic activity in xenograft mice model demonstrates that KBJK557-treated mice showed a considerable decrease in tumor size, proving the significances of Plk1 in lung cancer. Collectively, this study demonstrates that KBJK557 can serve as a promising drug candidate for treating the lung cancer through Plk1 PBD inhibition.

**Keywords:** Lung cancer, Polo-like kinase-1, Polo box domain, KBJK557, Inhibitor

## Introduction

Protein–protein interactions (PPI) play crucial roles in several biological processes. Dysfunction or abnormal regulation of PPI results in a range of diseases, including cancer. Thus, gaining insights into protein–protein interactions and their druggable sites can lead

to the identification of novel therapeutics. Polo-like kinases (Plks) are a class of serine/threonine protein kinases, classified into Plk1-5, which regulate cell cycle progression. In particular, during mitosis, Plk1 governs crucial roles including mitotic initiation, centrosome maturation, bipolar spindle formation, chromosome segregation, and cytokinesis (Luo et al. 2009). It is pertinent to note that Plk1 is dysregulated in a wide range of human tumors. Consequently, overexpression of Plk1 has been observed in various cancers, including ovarian, prostate, papillary thyroid, gastric, colorectal, pancreatic, head and neck, non-small cell lung cancers, melanoma, glioblastoma, and non-Hodgkin lymphoma (Chopra et al. 2010; Strebhardt and Ullrich 2006; Takai et al. 2005). A comparison of Plk1 levels between various cancers and normal tissues suggests that Lung squamous

†Pethaiah Gunasekaran and Gong-Hyeon Lee have contributed equally to this work

*Correspondence: mihyunkim@pusan.ac.kr; bangjk@kbsi.re.kr; ekryu@kbsi.re.kr

[1] Division of Bioconvergence Analysis, Korea Basic Science Institute (KBSI), Ochang, Chung Buk 28119, Republic of Korea
[2] Department of Internal Medicine, Pusan National University School of Medicine and Biomedical Research Institute, Pusan National University Hospital, Busan, Republic of Korea
Full list of author information is available at the end of the article

cell carcinoma, a type of non-small cell lung cancer (NSCLC), is one of the most Plk1 expressed cancers among the 19 cancer cells (Liu et al. 2017). A plethora of evidence suggests that specific interference of Plk1 induces mitotic arrest and subsequent apoptosis. Thus, it has been considered a potential drug target for anticancer therapy.

NSCLC is a kind of lung cancer that makes up 85% of lung cancers and includes squamous cell carcinomas, adenocarcinomas, and large-cell carcinomas (Bray et al. 2018). Lung cancer remains one of the most frequently diagnosed cancer, reporting 1.8 million new cases annually (Bray et al. 2018; Sung et al. 2021), and has the highest mortality rate among 36 cancer types worldwide with less than 20% of the average survival rate (Song et al. 2016). Most of the currently approved drugs for NSCLC are mainly targeting mutated proteins, including epidermal growth factor receptor (EGFR) family (ERBB-1, ERBB-2), TKI, ALK, ROS1, MET, RET, NTRK, and RAF (Rodak et al. 2021). However, drug resistance is the major challenge in the treatment of NSCLC. To overcome drug resistance in EGFR tyrosine kinase inhibitors (EGFR TKI), inhibition of Plk1 was found to be an effective strategy. For instance, combined inhibition of both Plk1 and EGFR induced apoptosis in EGFR TKIs-resistant NSCLC (Wang et al. 2016). It has been reported that inhibition of Plk1 downregulated STAT3 signaling, eventually suppressing the migration of A549 cancer cells (Yan et al. 2018). As Plk1 has been linked to tumor aggressiveness, inhibition of Plk1 is considered a valid strategy for drug discovery in NSCLC (Yan et al. 2018). Structurally, drug targeting site Plk1 is classified into two drug targeting sites, namely, the N-terminal kinase (KD) domain and the C-terminal polo-box domain (PBD). Employing KD inhibitors such as BI2536 and its successors, volasertib (BI 6727) showed significant effects against NSCLC cell proliferation (Choi et al. 2015) and drug-resistant NSCLC (Wang et al. 2016), respectively.

Although these two KD inhibitors advanced to clinical trials as Plk1 inhibitors, they were terminated during phase II and phase III clinical trials because of their toxicities and poor clinical benefits due to adverse effects. This may stem from cross-reactivity due to the homogeneity of ATP-binding pockets in various kinases (Rudolph et al. 2009). In contrast, the *C*-terminal PBD is a unique part of the Plk subfamily, and specific interference of Plk1 PBD is considered an attractive therapeutic strategy for treating cancer. As a result, peptide-based inhibitors, namely minimal peptide, PLHSpT, and its derivatives, were discovered with considerable potency and selectivity (Ahn et al. 2015). However, poor cell permeability and proteolytic stability are the most concerning factors for the evolution of peptide-based

inhibitors as drugs. To overcome these issues, several small-molecule-based-Plk1 PBD inhibitors, such as poloxin (Reindl et al. 2008), poloxin-2 (Scharow et al. 2015), poloxipan (Watanabe et al. 2009), purpurogallin (Watanabe et al. 2009), thymoquinone (Reindl et al. 2008), and green tea catechins (Shan et al. 2015) have been reported. However, these Plk1 PBD inhibitors have not been validated against NSCLC.

As part of anticancer drug discovery (Chirumarry et al. 2020; Gunasekaran et al. 2021), recently, we reported a pyrazolopyrimidine-fused small molecule, KBJK557, as a Plk1 PBD inhibitor with significant potency and selectivity (Gunasekaran et al. 2020). In vitro inhibition of Plk1 by KBJK557 induced cell cycle arrest and consecutive apoptosis. In addition, it showed remarkable cancer-targeting and treatment effects in xenograft mouse models with significant PKa profiles. Considering the above-mentioned Plk1 prominence in NSCLC and the potency of KBJK557, herein we evaluated the effect of KBJK557 on NSCLC cells, including A549, PC9, and H1975 cells for the first time. In vitro cell proliferation, cell cycle arrest, and apoptosis were studied along with in vivo experiments in mice models. This study contributes to an opening for NSCLC drug discovery through Plk1 PBD inhibition.
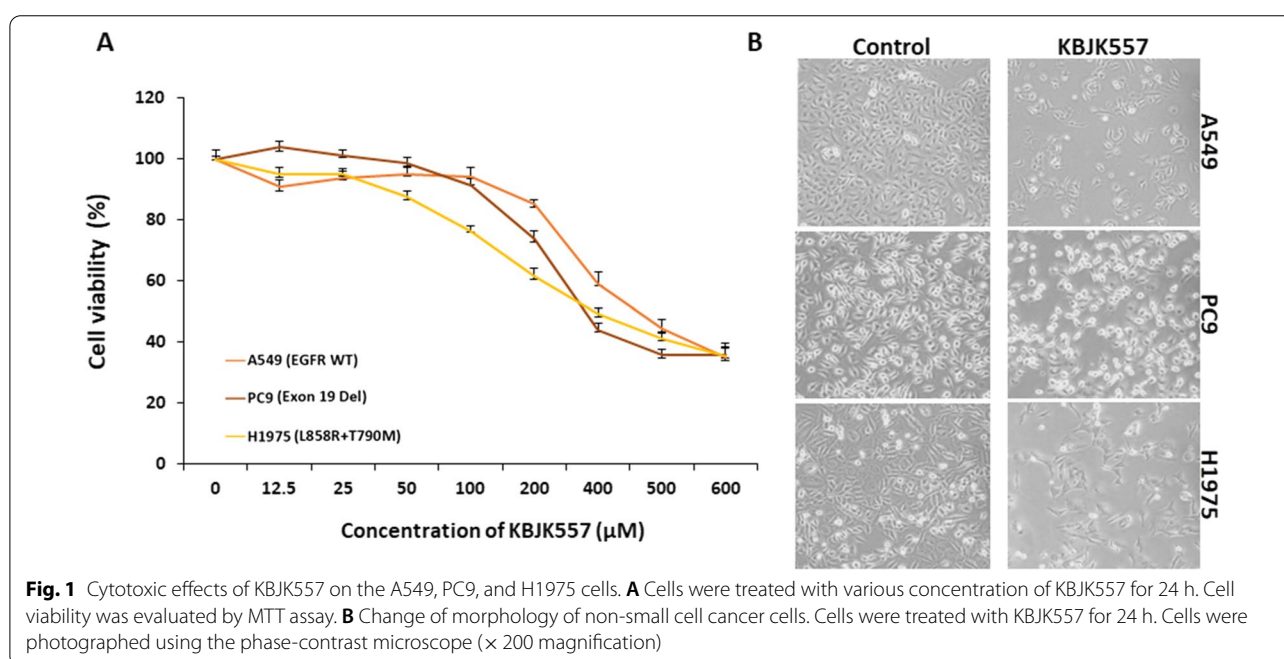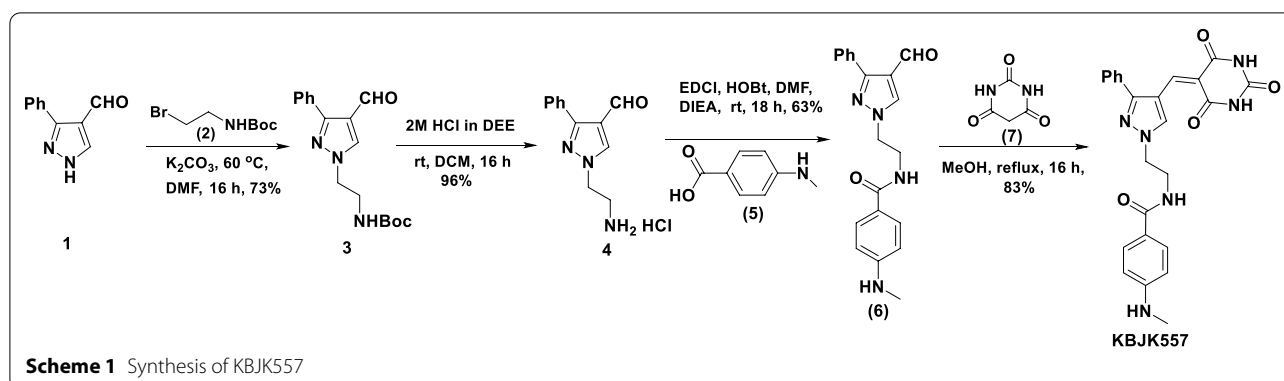
## Results

### Chemistry

Synthesis and detailed structure–activity relationship of KBJK557 are detailed in the reported procedure (Gunasekaran et al. 2020). Briefly, as delineated in Scheme 1, *N*-alkylation of 3-Phenyl-4-pyrazole carboxaldehyde (**1**) was performed using *N*-boc-bromoethylamine (**2**) in presence of potassium carbonate and DMF at 60 °C. Further treatment of 2M HCl with **3** resulted in the formation of the amine hydrochloride salt, **4**. Subsequently, 4-(methylamino)benzoic acid was coupled with amine hydrochloride (**4**) using EDC and HOBt in presence of DIEA in DMF to yield **6**, which was further treated with barbituric acid (6) in methanol under reflux conditions to obtain the desired compound, KBJK557 in good yield as shown below.

### Effect of KBJK557 on cell viability assay in NSCLC

To examine whether KBJK557 exhibits anticancer cell proliferation activity in vitro, we evaluated KBJK557 using the MTT assay using Plk1 expressed lung cancer cell lines, including A549, PC9, and H1975, as shown in Fig. 1. Each cancer cell line was incubated with various concentrations of KBJK557 for 24 h. Treatment with KBJK557 significantly decreased the cell viability in a dose-dependent manner. KBJK557 decreased the viability of A549, PC9, and H1975 cells with $IC_{50}$ values

**Scheme 1** Synthesis of KBJK557



**Fig. 1** Cytotoxic effects of KBJK557 on the A549, PC9, and H1975 cells. **A** Cells were treated with various concentration of KBJK557 for 24 h. Cell viability was evaluated by MTT assay. **B** Change of morphology of non-small cell cancer cells. Cells were treated with KBJK557 for 24 h. Cells were photographed using the phase-contrast microscope (× 200 magnification)

of 420, 350, and 400 µM, respectively. This was further confirmed by investigating the morphological changes in KBJK557-treated lung cancer cell lines (Fig. 1B). Treatment with KBJK557 substantially decreased the number of cancer cells, as shown in microscopic images.

### Effect KBJK557 on cell cycle arrest by fluorescence-activated cell sorting analysis

The effect of KBJK557 on cell cycle in non-small cell lung cancer cells progression was investigated using flow cytometry analysis. NSCLC cells were treated with KBJK557 for 24 h (Fig. 2). Notably, treatment with KBJK557 induced partial, but significant, G2/M phase arrest and delayed S-phase progression in all cell lines. For example, the population of A549 cells in the G1 phase decreased by 23%, whereas in S1 and G2/M stages, a substantial increase in cell count was observed

by approximately 10% and 12%, respectively. In contrast, PC9 cells showed a 4 and 36% decrease in cell counts at the G1 and S stages. However, these cells accumulated in the G2/M phase. In H1975 cells, KBJK557 caused a decrease in 16 counts that were populated at S and G2/M phases by 11 and 4 counts, respectively. These results indicated that KBJK557 inhibits the cell cycle in the G2/M phase of NSCLC cells.

### Apoptosis

Inspired by the significant G2/M arrest caused by KBJK557, we investigated the effect of KBJK557 on apoptosis in NSCLC cells, including A549, PC9, and H1975 (Fig. 3). Tumor cells were treated for 24 h with DMSO or KBJK557 (400 µM). In the fluorescence images, live cells and apoptotic cells are represented by red and green colors, respectively. KBJK557-treated samples exhibited
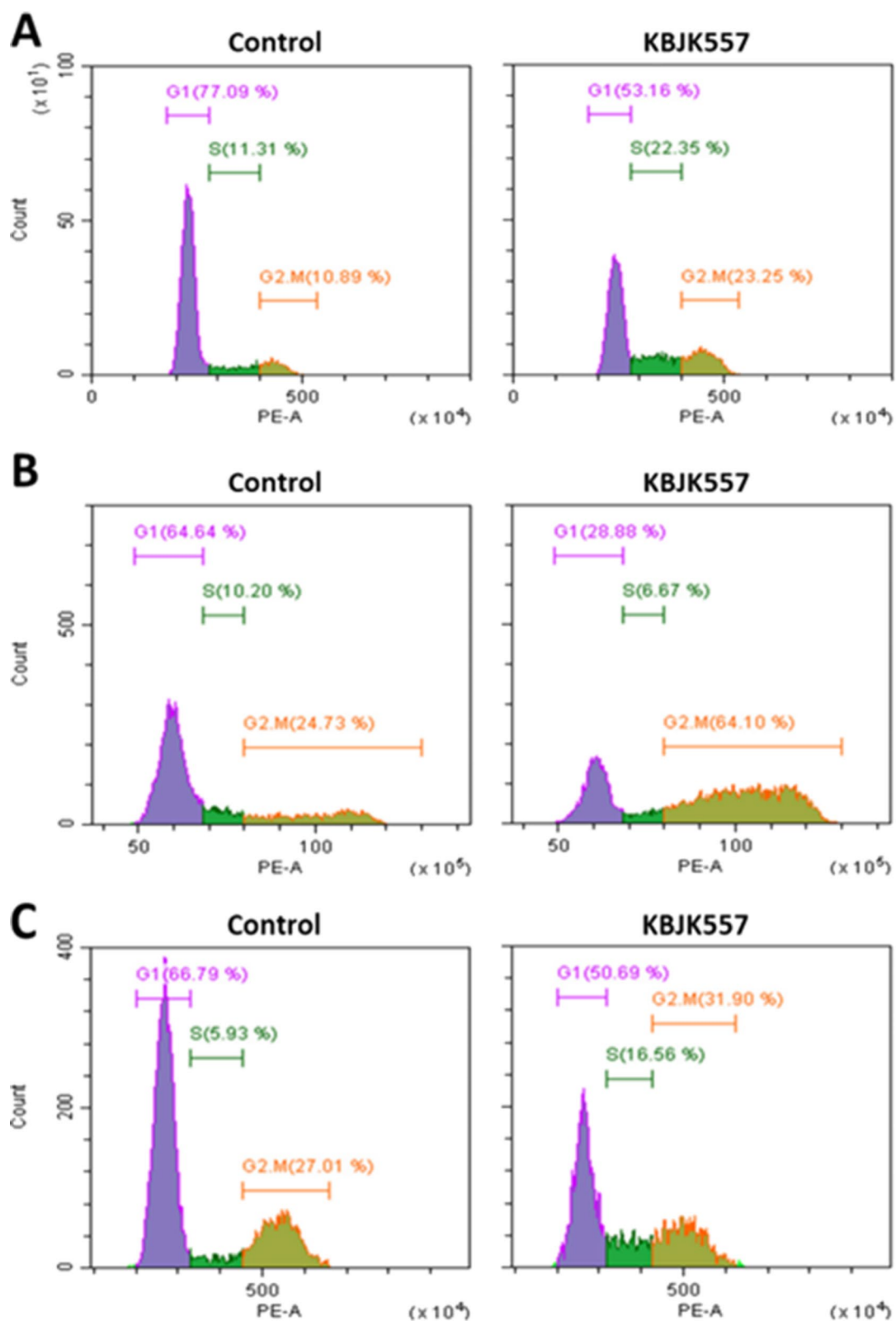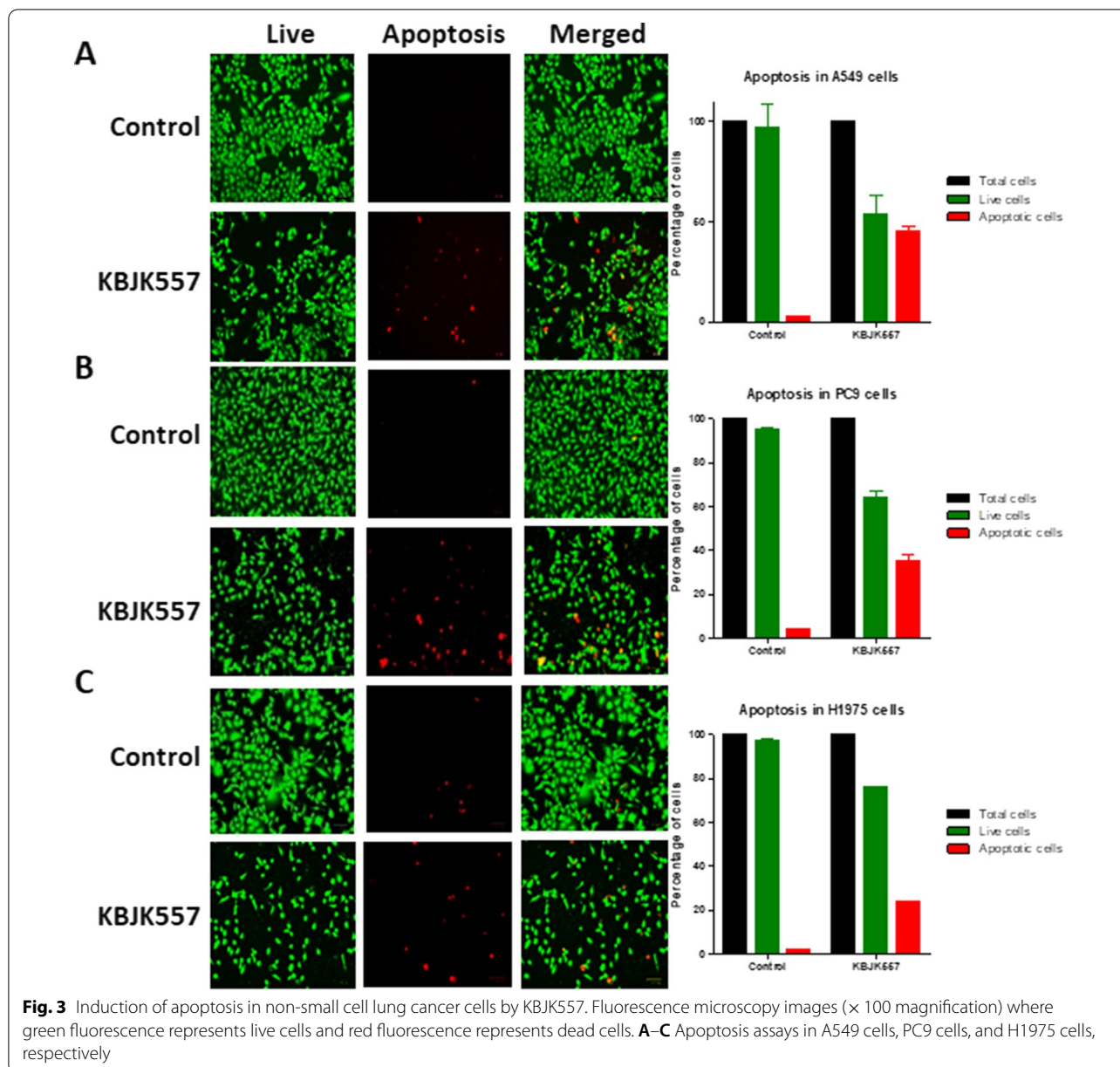
Gunasekaran *et al. Journal of Analytical Science and Technology* (2022) 13:36

Page 4 of 10



**Fig. 2** Fluorescence-activated cell sorting analysis of cell cycle arrest in non-small cell lung cancer cells after incubation with KBJK557 for 24 h. Cell cycle arrest was measured by flow cytometry with PI staining. **A** A549 cells. **B** PC9 cells. **C** H1975 cells
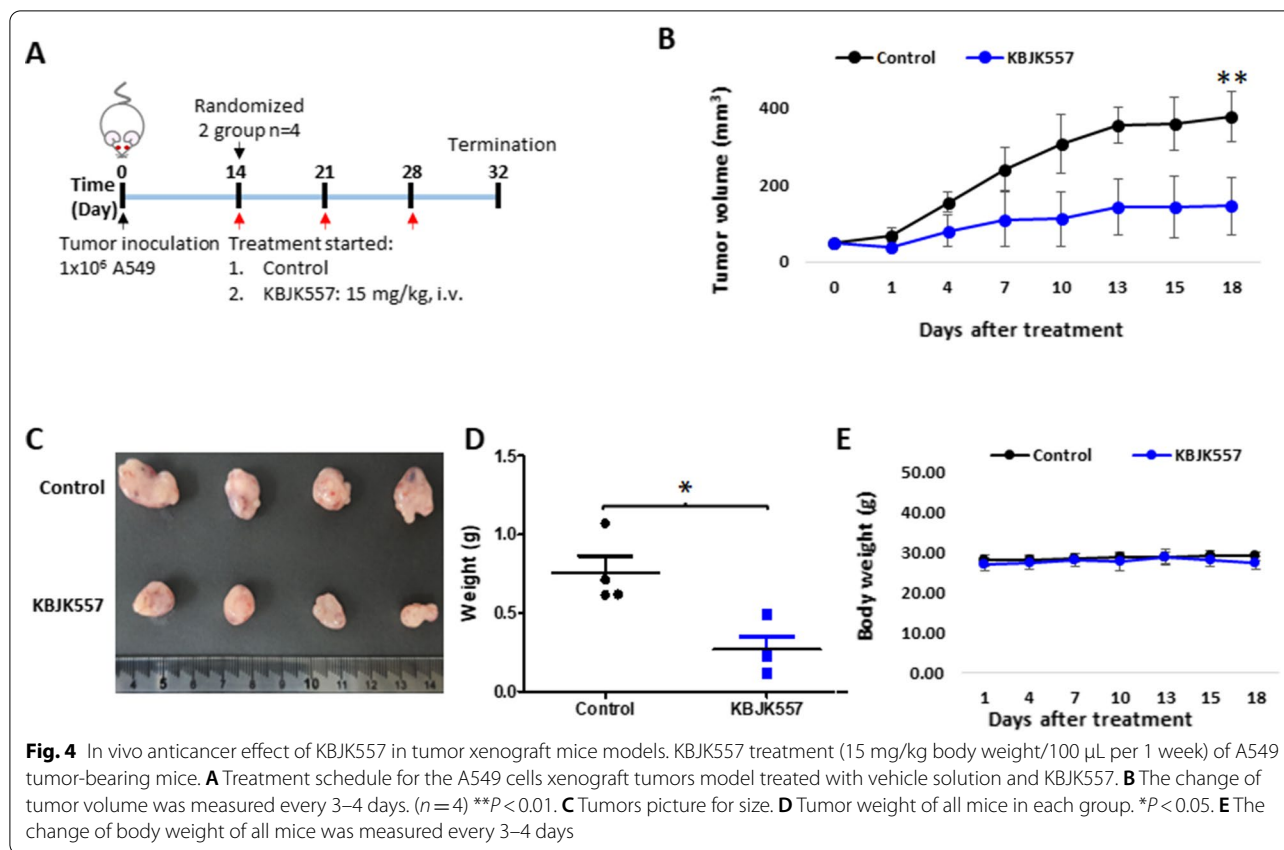
Gunasekaran *et al. Journal of Analytical Science and Technology*     (2022) 13:36

Page 5 of 10



**Fig. 3** Induction of apoptosis in non-small cell lung cancer cells by KBJK557. Fluorescence microscopy images (× 100 magnification) where green fluorescence represents live cells and red fluorescence represents dead cells. **A–C** Apoptosis assays in A549 cells, PC9 cells, and H1975 cells, respectively

cancer cell apoptosis of $57 \pm 6.5$, $24 \pm 0.2\%$, and $35 \pm 3\%$ at 400 μM against A549, PC9, and H1975 cells, respectively (Fig. 3A–C). The DMSO-treated groups exhibited apoptosis ($2.7 \pm 1.2$, $2 \pm 0.2\%$, and $4.4 \pm 0.1\%$, respectively). However, the proliferation of NSCLC cells was inhibited by KBJK557 due to the induction of apoptosis.

**Anticancer effect of KBJK557 on A549 tumor-bearing mice**
Inspired by the in vitro antitumor potential of KBJK557, we investigated its in vivo tumorigenic activity of KBJK557 in A549 tumor-bearing mice model (Fig. 4). Tumor xenograft mice were treated with KBJK557 and

PBS for 18 days ($n = 4$) (Fig. 4A). The control group exhibited a substantial increase in the number of cancer cells (Fig. 4B). In contrast, mice treated with KBJK557 showed a significant decrease in the number of cancer cells (Fig. 4B–D). To further ascertain whether the anticancer effect was entirely mediated by KBJK557, the body weights of mice in each group were measured (Fig. 4E). As shown in Fig. 4B, the body weights of mice treated with KBJK557 remained unaltered, confirmed that the decrease in tumor size was entirely due to the anticancer effect of KBJK557 and was not influenced by stress or environmental changes.

Gunasekaran *et al. Journal of Analytical Science and Technology*     (2022) 13:36

Page 6 of 10



**Fig. 4** In vivo anticancer effect of KBJK557 in tumor xenograft mice models. KBJK557 treatment (15 mg/kg body weight/100 µL per 1 week) of A549 tumor-bearing mice. **A** Treatment schedule for the A549 cells xenograft tumors model treated with vehicle solution and KBJK557. **B** The change of tumor volume was measured every 3–4 days. ($n=4$) **$P<0.01$. **C** Tumors picture for size. **D** Tumor weight of all mice in each group. *$P<0.05$. **E** The change of body weight of all mice was measured every 3–4 days

## Discussion

Plk1 facilitates tumor aggressiveness in various cancers, including NSCLC (Yan et al. 2018). Hence, inhibition of Plk1 is an attractive strategy for the discovery of anticancer drugs. Lung cancer remains one of the most commonly reported cancers worldwide with a significant number of occurrences and mortality rates. In particular, NSCLC accounts for a major portion of lung cancer reports. A combination of chemotherapy and platinum-based drugs has been used as first-line treatment for NSCLC. Second-line treatments included docetaxel, pemetrexed, and erlotinib. EGFRs are the most common therapeutic targets for NSCLC. Second- and third-line patients were treated with gefitinib which targets EGFR. Although significant improvements in survival rates have been reported for erlotinib and gefitinib treatments, acquiring drug resistance is inevitable (Song et al. 2016). Alternatively, achieving mitotic arrest by targeting mitotic regulatory proteins or kinases is a valid approach to overcome drug resistance. For instance, Plk1 is such a target that plays key roles in cell cycle events. Thus, evaluation of the Plk1 inhibitor, volasertib against NSCLC suggests that it serves as a tool to overcome erlotinib resistance in the T790M mutation. In addition, combined inhibition of both Plk1 and EGFR facilitated

apoptosis, proving the prominence of Plk1 in NSCLC (Wang et al. 2016). Similarly, BI2536 exerts cytotoxic effects in human lung cancer cell lines (Steegmaier et al. 2007), and also showed cytotoxic effects in elevated p53 in A549 cells (Sanhaji et al. 2012). The mechanistic investigation suggests that cell death was triggered through mitotic catastrophe which is a type of cell death that occurs after mitotic arrest (Choi et al. 2015). GSK461364, HMN-176, and ON 01910.Na (rigosertib) are another few Plk1 inhibitors that exert cytotoxic effects against NSCLC cells (Medema et al. 2011).

Although these Plk1 KD inhibitors showed prominent effects in NSCLC, similarities in the ATP-binding pockets led to cross-reactivity, leading to undesirable side effects. Thus, targeting PBD of Plk1 is a valuable tool for addressing those side effects. Several potent peptide-based Plk1 PBD have been successfully derived, however, their potency is limited at the cell level and its advancement is hampered by poor cell permeability and proteolytic cleavages. Our recent report demonstrates the discovery of a Plk1 PBD inhibitor KBJK557 that displayed a significant antitumorigenic activity in mice model through inhibition of Plk. And the in vitro anticancer effect was facilitated through cell cycle arrest, apoptosis with significant Pk profile (Gunasekaran et al.

2020). Considering, the importance of Plk1 in NSCLC and potency of KBJK557, in this report we evaluated KBJK557 against NSCLC cancer cell lines. Interestingly, KBJK557 displayed notable cytotoxic effects in A549, PC9, and H1975 cells. The observed slight elevation in the inhibitory concentrations is due to limited solubility, which is the major challenge faced by the majority of anticancer drugs currently in pipeline. However, these drugs cannot be ruled out because of their prominent potency (Sawicki et al. 2016). For instance, rapamycin shows promising anticancer activity but has poor solubility. Approximately 65% of the existing approved anticancer drugs suffer from poor solubility to achieve maximum therapeutic outcomes (Sawicki et al. 2016). In this regard, in KBJK557, when solubility issue is overcome, achieving significant inhibitory concentrations becomes more likely. Further investigation of the cell cycle suggests that KBJK557-treated cells show a significant increase in population in the G2/M stage while depleting at the G1 stage, demonstrating the influence of KBJK557 on cell cycle arrest in NSCLC cells through Plk1 inhibition. As a result of cell cycle arrest, KBJK557 significantly induced apoptosis in the A549, PC9, and H1975 cells. In particular, A549 cells showed the maximum apoptotic effect. An in vivo anticancer evaluation of KBJK557 in A549 tumor-bearing mice model suggested that KBJK557 can inhibit tumor growth by approximately 60%. It is pertinent to note that BI2536 revealed the maximum in vivo efficacy in A549 while using 50 mg/kg (Steegmaier et al. 2007). However, KBJK557 displayed a significant antitumorigenic effect at 15 mg/kg, proving the prominent effect of KBJK557 over Plk1 KD inhibitors.

## Conclusion

Non-small cell lung cancer (NSCLC) is one of the most commonly reported cancers worldwide. NSCLC shows elevated levels of Plk1 expressions, which is considered an attractive drug target in many cancers. Very few Plk1 KD inhibitors have been reported to show notable potency against NSCLC. However, side effects due to cross-reactivity with similar kinases and selectivity are the key challenges associated with these inhibitors. To overcome these challenges, we validated the recently reported Plk1 PBD inhibitor, KBJK557, against NSCLC cells. KBJK557 showed significant in vitro anticancer effects through cell cycle arrest and subsequent apoptosis. Furthermore, evaluation of in vivo antitumorigenic activity in xenograft mouse models demonstrated that KBJK557 has immense potential to evolve as a model for designing NSCLC drugs. To the best of our knowledge, KBJK557 is the first small-molecule Plk1 PBD inhibitor to show significant in vitro and in vivo anticancer effects against NSCLC.

## Materials and methods

KBJK557 was synthesized according to the procedure (Gunasekaran et al. 2020), and the experimental section is provided in Additional file 1. As described previously (Gunasekaran et al. 2017), all reactions were performed under argon atmosphere in flame-dried glassware using dry solvents, unless otherwise noted. Anhydrous organic solvents (99.9%) were purchased from Sigma-Aldrich and used in the reaction. Sigma- All reagents and few starting materials were purchased from Aldrich, TCI, and Across Organics and utilized in the reaction. Merck aluminum sheets with silica gel 60 F254 using 0.25 mm plates were used for thin-layer chromatography (TLC) and visualized by ultraviolet light, staining with phosphomolybdic acid (PMA), $KMnO_4$, and ninhydrin. Merck silica gel 60 (70–230 mesh or 230–400 mesh) was used for column chromatography purification. Bruker DRX-400 and DRX-500 NMR spectrometers were used to record $^1$H and $^{13}$C NMR spectra. NMR chemical shifts (δ) are denoted in parts per million (ppm) and coupling constants (J) are given in hertz (Hz) (Additional file 1: Supplementary Information). MALDI-TOF mass was recorded using a Shimadzu mass spectrometer.

### *Tert*-butyl (2-(4-formyl-3-phenyl-1*H*-pyrazol-1-yl)ethyl) carbamate (3)

3-phenyl-1*H*-pyrazole-4-carbaldehyde (**1**) (0.5 g, 2.906 mmol) in anhydrous DMF (5 mL) was added slowly to a stirred solution of *tert*-butyl (2-bromoethyl) carbamate (**2**) (0.604 g, 2.642 mmol) and potassium carbonate (1.47 g, 7.90 mmol) in anhydrous DMF (10 mL). After completion of the addition, the temperature was slowly raised to 60 °C and stirred for 16 h. The reaction mixture was quenched by the addition of water (20 mL) and extracted with ethyl acetate (20 mL × 3). The combined organic extracts were washed with brine (40 mL), dried over $Na_2SO_4$, and evaporated. The crude product was purified by trituration using DCM-hexane to yield **3** as a white solid (0.67 g, 73%). $^1$H NMR (500 MHz, $CDCl_3$) δ 9.98 (s, 1H), 8.04 (s, 1H), 7.75 (d, $J = 6.8$ Hz, 2H), 7.56–7.41 (m, 3H), 4.87 (s, 1H), 4.34 (s, 2H), 3.75–3.58 (m, 2H), 1.47 (s, 9H). $^{13}$C NMR (101 MHz, $CDCl_3$) δ 185.2, 154.6, 150.3, 138.4, 134.8, 131.4, 130.1, 129.1, 128.8, 120.9, 120.3, 80.2, 52.4, 40.4, 28.3.

### 1-(2-aminoethyl)-3-phenyl-1*H*-pyrazole-4-carbaldehyde hydrochloride (4)

2 M HCl (11 mL, 22 mmol) in diethyl ether was added to the stirred solution of **3** (700 mg, 2.22 mmol) in 10 mL dichloromethane. The resultant solution was stirred for 16 h at rt and the solid formed was filtered and washed with anhydrous diethyl ether to yield **4** as pale-yellow

solid (537 mg, 96%). $^1H$ NMR (400 MHz, DMSO-$d_6$) δ 9.89 (s, 1H), 8.66 (s, 1H), 8.64–8.36 (m, 3H), 7.90–7.79 (m, 2H), 7.51–7.34 (m, 3H), 4.58 (d, $J=6.1$ Hz, 2H), 3.34 (q, $J=5.8$ Hz, 2H). $^{13}C$ NMR (101 MHz, DMSO-$d_6$) δ 185.0, 152.6, 138.7, 132.1, 129.3, 129.1, 128.9, 121.0, 49.5, 38.7. Maldi-tof m/z calcd for $C_{12}H_{13}N_3O$: 215.10, found 215.44.

### *N*-(2-(4-formyl-3-phenyl-*1H*-pyrazol-1-yl) ethyl)-4-(methylamino)benzamide (6)

To a stirred solution of EDCI (607 mg, 3.18 mmol), HOBt (428 mg, 3.18 mmol) in DMF (10 mL), 4-(methyl-amino)benzoic acid (**5**) (480 mg, 3.18 mmol) and DIEA (2.76 mL, 15.86 mmol) was added and stirred for 30 min. To the resultant solution, **4** (957 mg, 3.81 mmol) in DMF (5 mL) was added and allowed to stir at rt for 18 h. The reaction mixture was treated with 5% $NaHCO_3$ solution (20 mL) and extracted with ethyl acetate ($2 \times 15$ mL), the combined organic layer was washed with $H_2O$ and brine, dried over $Na_2SO_4$, and evaporated under vacuum. The crude residue was purified by flash column chromatography ($CH_2Cl_2$/ethyl acetate (3:1)) to provide **6** (0.834 g, 63%) as semi-solid. $^1H$ NMR (400 MHz, $CDCl_3$) δ 9.89 (s, 1H), 7.96 (s, 1H), 7.74 (dd, $J=7.6$, 1.8 Hz, 2H), 7.60 (d, $J=8.7$ Hz, 2H), 7.52–7.39 (m, 3H), 6.80 (t, $J=5.2$ Hz, 1H), 6.52 (d, $J=8.7$ Hz, 2H), 4.47–4.33 (m, 2H), 4.17 (s, 1H), 3.90 (q, $J=5.6$ Hz, 2H), 2.85 (s, 3H). $^{13}C$ NMR (101 MHz, $CDCl_3$) δ 184.8, 167.7, 154.3, 152.1, 135.2, 131.5, 129.1, 128.8, 128.7, 121.7, 120.88, 111.4, 52.1, 39.9, 30.2. (traces of dichloromethane are present). Maldi-tof m/z calcd for $C_{20}H_{20}N_4O_2$: 348.15, found 348.77, 360.76 (M+Na) $^+$.

### 4-(methylamino)-N-(2-(3-phenyl-4-((2,4,6-trioxotetrahy-dropyrimidin-5(2H)-ylidene)methyl)-1H-pyrazol-1-yl)ethyl) benzamide (KBJK557)

Barbituric acid (**7**) (0.269 g, 2.1 mmol) was added to a stirred solution of **6** (800 mg, 2.3 mmol) in dry methanol (15 mL) and heated to reflux for 16 h. The resultant yellow solid was filtered and washed with cold methanol ($3 \times 5$ mL) and dried to yield a pure compound, KBJK557 as a yellow solid (798 mg, 83%). $^1H$ NMR (400 MHz, DMSO-$d_6$) δ 11.19 (s, 2H), 9.32 (s, 1H), 8.23 (t, $J=5.4$ Hz, 1H), 8.15 (s, 1H), 7.70–7.40 (m, 7H), 6.51 (d, $J=8.7$ Hz, 2H), 6.19 (q, $J=4.7$ Hz, 1H), 4.47 (t, $J=5.8$ Hz, 2H), 3.70 (q, $J=5.8$ Hz, 2H), 2.71 (d, $J=4.9$ Hz, 3H). $^{13}C$ NMR (101 MHz, DMSO-$d_6$) δ 167.2, 164.3, 163.2, 157.8, 152.7, 150.7, 144.9, 139.0, 131.7, 130.0, 129.5, 129.2, 129.2, 121.1, 113.8, 112.9, 110.8, 52.2, 40.6, 40.4, 40.2, 40.1, 39.8, 39.6, 39.5, 29.8. Maldi-tof m/z calcd for $C_{24}H_{22}N_6O_4$: 458.17, found 458.74.

### Cell viability assay

As reported previously (Gunasekaran et al. 2020), human lung cancer cells (A549, PC9, and H1975) were purchased from the Korean Cell Line Bank (Seoul, Korea), Sigma-Aldrich (Missouri, USA) and ATCC (Virginia, USA). Lung cancer cells were propagated in RPMI 1640 medium (Cytiva, USA), supplemented with 10% fetal bovine serum (FBS, Hyclone, USA), and 1% of penicillin–streptomycin (Sigma-Aldrich, USA) at 37 °C in a humidified incubator with 5% $CO_2$. Lung cancer cells were seeded at a density of $1 \times 10^3$ cells per 96-well plates in 100 μL medium. After 24 h of incubation, Lung cancer cells were treated with KBJK557 at various concentrations (0, 12.5, 25, 50, 100, 200, 400, 500, and 600 μM) for 24 h, then added to the MTT assay (Enhanced Cell Viability Assay Kit, DoGenBio, Korea). Absorbance was measured at 450 nm using a microplate reader (Molecular Devices Corp, USA).

### Cell cycle arrest study by fluorescence-activated cell sorter

As reported previously (Gunasekaran et al. 2020), lung cancer cells were seeded into $2 \times 10^5$ cells in 6-well plates and treated with KBJK557 (400 μM) for 24 h. Cells were washed with PBS three times and fixed using 70% cold ethanol during vortexing. The fixed cells were stained with propidium iodide (PI) (1 μg/mL, Sigma-Aldrich, USA) and treated RNase (1 μg/mL) (Thermo Scientific, USA) in PBS for 30 min at 37 °C in an incubator. Flow cytometric analysis was performed using a fluorescence-activated cell sorter (FACS; Beckman Coulter, CytoFLEX, USA).

### Apoptosis effect of cancer cells

As reported previously (Gunasekaran et al. 2020), lung cancer cells ($1 \times 10^3$ cells) were cultured in 96-well microplates for 24 h at 37 °C. Cells were treated with KBJK557 (400 μM) at 24 h. Then, 2.5 μL of mixtures of kit (LIVE/DEAD™ Viability/Cytotoxicity Kit, Invitrogen™, USA) were added to 1 mL of PBS, and 100 μL of this solution was added to each well. After 30 min of incubation at room temperature, images of cells were captured by fluorescence microscope (ZOE™ Fluorescent Cell Imager, USA). Cells count was measured using ImageJ software.

### Animals

As reported previously (Gunasekaran et al. 2020), five-week-old male BALB/c nude mice were purchased from the Nara Bio animal center (NARA Biotech, Seoul, Korea), housed under specific pathogen-free conditions. The mice were housed in groups of four in transparent plastic cages bedded with aspen chip and were provided with standard mouse chow diet and tap water ad libitum when not being treated. The environment of the animal room was carefully controlled, with a 12 h dark–light cycle. And the

Gunasekaran *et al. Journal of Analytical Science and Technology*     (2022) 13:36

Page 9 of 10

temperature was maintained around 20–21 °C with relative humidity of 40–45%. The animal experiments were carried out according to a protocol approved by the KBSI Committee (KBSI-IACUC-22-6) and all experiments were performed in accordance with relevant guidelines and regulations.

### The anticancer effect in tumor-bearing mice
As reported previously (Gunasekaran et al. 2020), we induced mouse xenograft tumor models by subcutaneously injecting $1 \times 10^6$ A549 cells in PBS into the right thigh region of six-week-old male BALB/c nu/nu mice. When the tumor volume (length × width × height × 0.52, mm$^3$) reached approximately 50 mm$^3$, a tail vein injection of vehicle solution, and KBJK557 (15 mg/kg) was carried out. KBJK557 was dissolved in Dimethyl sulfoxide (DMSO, Sigma-Aldrich, USA), Polyethylene glycol 300 (PEG300, Selleck Chemical, USA), Tween 80 (Fluka, Switzerland), and distilled water (D.W.) (5:30:5:60, v/v/v/v, 100 μL). We injected vehicle solution and KBJK557 at 3–4 day intervals for 18 days and the tumor size was measured using calipers.

## Supplementary Information
The online version contains supplementary material available at https://doi.org/10.1186/s40543-022-00345-2.

**Additional file 1.** Supplementary information.

## Declarations

### Competing interests
The authors declare no competing interests.

### Author details
[1]Division of Bioconvergence Analysis, Korea Basic Science Institute (KBSI), Ochang, Chung Buk 28119, Republic of Korea. [2]Department of Internal Medicine, Pusan National University School of Medicine and Biomedical Research Institute, Pusan National University Hospital, Busan, Republic of Korea. [3]Department of Bio-analytical Science, University of Science and Technology, Daejeon 34113, Republic of Korea. [4]Dandicure Inc, Ochang, Chung Buk 28119, Republic of Korea.

## References
Ahn M, Han YH, Park JE, Kim S, Lee WC, Lee SJ, Gunasekaran P, Cheong C, Shin SY Sr, Kim HY, Ryu EK, Ryu EK, Murugan RN, Kim N-H, Bang JK. A new class of peptidomimetics targeting the polo-box domain of polo-like kinase 1. J Med Chem. 2015;58(1):294–304. https://doi.org/10.1021/jm501147g.
Bray F, Ferlay J, Soerjomataram I, Siegel RL, Torre LA, Jemal A. Global cancer statistics 2018: GLOBOCAN estimates of incidence and mortality worldwide for 36 cancers in 185 countries. CA A Cancer J Clin. 2018;68(6):394–424.
Chirumarry S, Soung NK, Han J, Kim EY, Ryu EK, Lee YH, Shin SY, Gunasekaran P, Bang JK. Antibacterial AZT derivative regulates metastasis of breast cancer cells. Eur J Med Chem. 2020;193:112233. https://doi.org/10.1016/j.ejmech.2020.112233.
Choi M, Kim W, Cheon MG, Lee CW, Kim JE. Polo-like kinase 1 inhibitor BI2536 causes mitotic catastrophe following activation of the spindle assembly checkpoint in non-small cell lung cancer cells. Cancer Lett. 2015;357(2):591–601.
Chopra P, Sethi G, Dastidar SG, Ray A. Polo-like kinase inhibitors: an emerging opportunity for cancer therapeutics. Expert Opin Investig Drugs. 2010;19(1):27–43. https://doi.org/10.1517/13543780903483191.
Gunasekaran P, Lee S-R, Jeong S-M, Kwon J-W, Takei T, Asahina Y, Bang G, Kim S, Ahn M, Ryu EK, Kim HN, Nam K-Y, Shin SY, Hojo H, Namgoong S, Kim N-H, Bang JK. Pyrrole-based macrocyclic small-molecule inhibitors that target oocyte maturation. ChemMedChem. 2017;12(8):580–9. https://doi.org/10.1002/cmdc.201700048.
Gunasekaran P, Yim MS, Ahn M, Soung NK, Park JE, Kim J, Bang G, Shin SC, Choi J, Kim M, Kim HN, Kim Y-H, Chung Y-H, Lee K, Kim EEK, Jeon Y-O, Kim MJ, Lee K-R, Kim B-Y, Lee KS, Ryu EK, Bang JK. Development of a polo-like kinase-1 polo-box domain inhibitor as a tumor growth suppressor in mice models. J Med Chem. 2020;63(23):14905–20. https://doi.org/10.1021/acs.jmedchem.0c01451.
Gunasekaran P, Han HJ, Choi JH, Ryu EK, Park NY, Bang G, La YK, Park S, Hwang K, Kim HN, Kim MH, Jeon YH, Soung N-K, Bang JK. Amphipathic Small Molecule AZT compound displays potent inhibitory effects in cancer cell proliferation. Pharmaceutics. 2021. https://doi.org/10.3390/pharmaceutics13122071.
Liu Z, Sun Q, Wang X. PLK1, a potential target for cancer therapy. Transl Oncol. 2017;10(1):22–32.
Luo J, Emanuele MJ, Li D, Creighton CJ, Schlabach MR, Westbrook TF, Wong K-K, Elledge SJ. A genome-wide RNAi screen identifies multiple synthetic lethal interactions with the Ras oncogene. Cell. 2009;137(5):835–48.
Medema RH, Lin C-C, Yang JC-H. Polo-like kinase 1 inhibitors and their potential role in anticancer therapy, with a focus on NSCLC. Clin Cancer Res. 2011;17(20):6459–66.
Reindl W, Yuan J, Krämer A, Strebhardt K, Berg T. Inhibition of polo-like kinase 1 by blocking polo-box domain-dependent protein-protein interactions. Chem Biol. 2008;15(5):459–66. https://doi.org/10.1016/j.chembiol.2008.03.013.
Rodak O, Peris-Díaz MD, Olbromski M, Podhorska-Okołów M, Dzięgiel P. Current landscape of non-small cell lung cancer: epidemiology, histological classification, targeted therapies, and immunotherapy. Cancers. 2021. https://doi.org/10.3390/cancers13184705.
Rudolph D, Steegmaier M, Hoffmann M, Grauert M, Baum A, Quant J, Haslinger C, Garin-Chesa P, Adolf GR. BI 6727, a polo-like kinase inhibitor with improved pharmacokinetic profile and broad antitumor activity. Clin Cancer Res. 2009;15(9):3094–102. https://doi.org/10.1158/1078-0432.CCR-08-2445.
Sanhaji M, Kreis N-N, Zimmer B, Berg T, Louwen F, Yuan J. p53 is not directly relevant to the response of polo-like kinase 1 inhibitors. Cell Cycle. 2012;11(3):543–53. https://doi.org/10.4161/cc.11.3.19076.
Sawicki E, Schellens JH, Beijnen JH, Nuijen B. Inventory of oral anticancer agents: pharmaceutical formulation aspects with focus on the solid dispersion technique. Cancer Treat Rev. 2016;50:247–63. https://doi.org/10.1016/j.ctrv.2016.09.012.

Scharow A, Raab M, Saxena K, Sreeramulu S, Kudlinzki D, Gande S, Dötsch C, Kurunci-Csacsko E, Klaeger S, Kuster B, Schwalbe H, Strebhardt K, Berg T. Optimized Plk1 PBD inhibitors based on poloxin induce mitotic arrest and apoptosis in tumor cells. ACS Chem Biol. 2015;10(11):2570–9. https://doi.org/10.1021/acschembio.5b00565.

Shan H-M, Shi Y, Quan J. Identification of green tea catechins as potent inhibitors of the polo-box domain of polo-like kinase 1. ChemMedChem. 2015;10(1):158–63. https://doi.org/10.1002/cmdc.201402284.

Song Z, Ge Y, Wang C, Huang S, Shu X, Liu K, Zhou Y, Ma X. Challenges and perspectives on the development of small-molecule EGFR inhibitors against T790M-mediated resistance in non-small-cell lung cancer. J Med Chem. 2016;59(14):6580–94. https://doi.org/10.1021/acs.jmedchem.5b00840.

Steegmaier M, Hoffmann M, Baum A, Lénárt P, Petronczki M, Krššák M, Gürtler U, Garin-Chesa P, Lieb S, Quant J, Grauert M, Adolf GR, Kraut N, Peters J-M, Rettig WJ. BI 2536, a potent and selective inhibitor of polo-like kinase 1, inhibits tumor growth in vivo. Curr Biol. 2007;17(4):316–22. https://doi.org/10.1016/j.cub.2006.12.037.

Strebhardt K, Ullrich A. Targeting polo-like kinase 1 for cancer therapy. Nat Rev Cancer. 2006;6(4):321–30. https://doi.org/10.1038/nrc1841.

Sung H, Ferlay J, Siegel RL, Laversanne M, Soerjomataram I, Jemal A, Bray F. Global cancer statistics 2020: GLOBOCAN estimates of incidence and mortality worldwide for 36 cancers in 185 countries. CA Cancer J Clin. 2021;71(3):209–49. https://doi.org/10.3322/caac.21660.

Takai N, Hamanaka R, Yoshimatsu J, Miyakawa I. Polo-like kinases (Plks) and cancer. Oncogene. 2005;24(2):287–91. https://doi.org/10.1038/sj.onc.1208272.

Wang Y, Singh R, Wang L, Nilsson M, Goonatilake R, Tong P, Li L, Giri U, Villalobos P, Mino B, Rodriguez-Canales J, Wistuba I, Wang J, Heymach JV, Johnson FM. Polo-like kinase 1 inhibition diminishes acquired resistance to epidermal growth factor receptor inhibition in non-small cell lung cancer with T790M mutations. Oncotarget. 2016;7(30):47998–8010. https://doi.org/10.18632/oncotarget.10332.

Watanabe N, Sekine T, Takagi M, Iwasaki J-I, Imamoto N, Kawasaki H, Osada H. Deficiency in chromosome congression by the inhibition of Plk1 polo box domain-dependent recognition*. J Biol Chem. 2009;284(4):2344–53. https://doi.org/10.1074/jbc.M805308200.

Yan W, Yu H, Li W, Li F, Wang S, Yu N, Jiang Q. Plk1 promotes the migration of human lung adenocarcinoma epithelial cells via STAT3 signaling. Oncol Lett. 2018;16(5):6801–7. https://doi.org/10.3892/ol.2018.9437.

## Publisher's Note